Supplement of Atmos. Meas. Tech., 9, 1685–1699, 2016
http://www.atmos-meas-tech.net/9/1685/2016/
doi:10.5194/amt-9-1685-2016-supplement

Atmospheric Measurement Techniques
Open Access
EGU

Supplement of

Interannual variability of temperature in the UTLS region over Ganges–Brahmaputra–Meghna river basin based on COSMIC GNSS RO data

Joseph L. Awange and Ehsan Forootan

Correspondence to: Khandu (khandu@postgrad.curtin.edu.au)

1 Outline

The accuracy of IMD radiosondes have been a concern for many years due to their poor performance (see, e.g., *Das Gupta et al.*, 2005; *Kumar et al.*, 2011; *Sun et al.*, 2010; *Ansari et al.*, 2015) and has undergone major upgrades in the past 5-6 years. A detailed evaluation of 12 sonde types globally by *Sun et al.* (2010) from April 2008 to October 2009 showed that radiosonde observations over India (MK4) were found to be significantly biased when compared to COSMIC RO data while those over China (ShangE/M) suffered from large negative refractivity biases in the mid-troposphere. However, *Kumar et al.* (2011); *Ansari et al.* (2015) reported significant reduction in daily temperature fluctuations at 10 stations over India, which were prominent before they were upgraded. Therefore, improvements are expected mainly in the humidity measurements, which are represented by water vapour pressure.

This supplementary material contains information on the quality of temperature, water-vapour pressure, and refractivity profiles obtained from radiosonde stations within the GBM River Basin. We use an extended period of COSMIC RO data (wet profiles) to evaluate the accuracy of radiosonde measurements over the GBM River Basin. Radiosonde stations are located mainly over India (18), China (3), and Bangladesh (3). The quality of these three variables were examined using COSMIC RO profiles that are collocated within a radius of 200 km and 2 hours time difference over the period August 2006 to December 2013.

The geostatistial kriging method that is used to interpolate COSMIC RO data based on monthly accumulated RO data is also discussed here.

2 Radiosonde Data

Besides RO data, CDAAC also maintains an archive of radiosonde records from around the globe that are collocated with the RO profiles (e.g., COSMIC, CHAMP, GRACE). These radiosonde records are extracted from National Center for Atmospheric Research (NCAR) mass store (see details in, *Sun et al.*, 2010). In this evaluation, 24 operational or synoptic radiosonde stations within or around the GBM Basin were considered. The location of these statios are shown in Figure S1 including their design types. Among them, 18 stations are located within the Indian territory and are operated by the the Indian Meteorological Department (IMD) (see, Figure S1). Three radiosonde stations are located in China (or the upper Brahmaputra basin), and the remaining three are located in Bangladesh. Based on the country of location, these radiosondes differ in their sensor types. The details of the radiosondes are provided in Table S1.

3 Comparison Methods

The two data sets (radiosonde and COSMIC RO) are carried out at 13 standard pressure levels (i.e., 850 hPa, 700 hPa, 500 hPa, 400 hPa, 300 hPa, 250 hPa, 200 hPa, 150 hPa, 100 hPa, 70 hPa, 50 hPa, 30 hPa, and 20 hPa) for temperature (T), water vapour pressure (p_w), and refractivity (R). The errors (or biases) are expressed relative to the COSMIC RO data in terms of temperature differences (ΔT) and relative errors of water vapour pressure (RE p_w) and refractivity (RE N) at various pressure levels based on Eq. 1-3 as shown below:

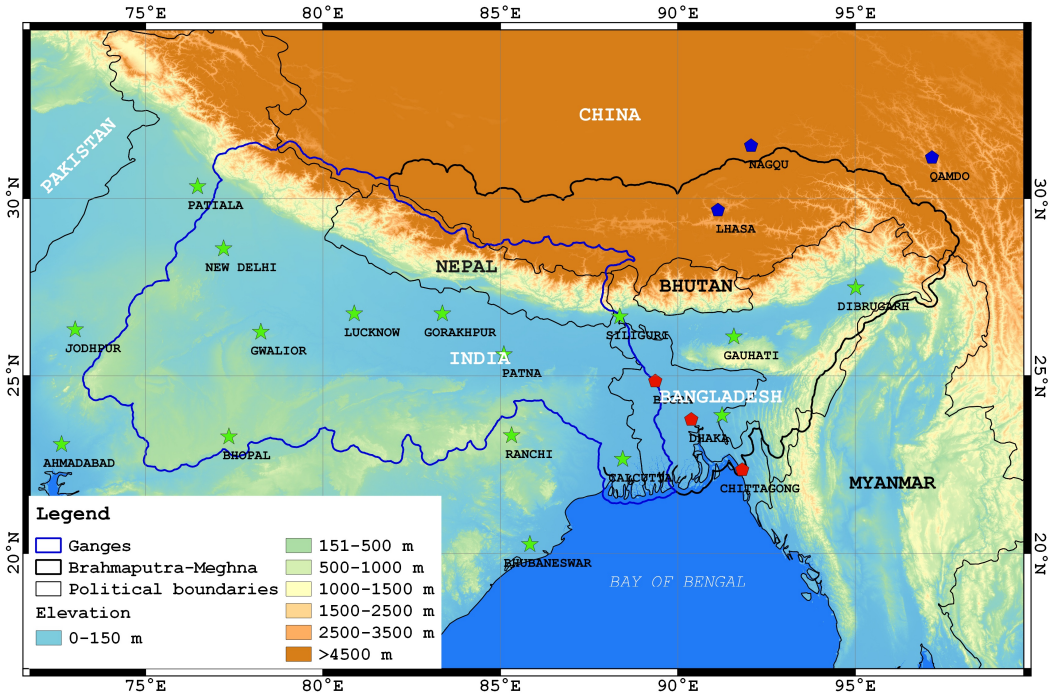

Figure S1: Elevation of the Ganges-Brahmaputra-Meghna Basin in South Asia. The digital elevation model is derived from the Shuttle Radar Topography mission (SRTM, http://srtm.csi.cgiar.org). The locations of the radiosonde stations are shown in different colors, green for those over India (IMD/MK4), red for those over Bangladesh (Bdesh), and blue for those over China (ShangE/M) and their details are shown in Table S1.

$$\Delta\, T = T^{\text{radiosonde}} - T^{\text{COSMIC}} \tag{1}$$

$$\text{RE}\ p_w = \frac{p_w^{\text{radiosonde}} - p_w^{\text{COSMIC}}}{p_w^{\text{COSMIC}}} \tag{2}$$

$$\text{RE}\ N = \frac{N^{\text{radiosonde}} - N^{\text{COSMIC}}}{N^{\text{COSMIC}}} \tag{3}$$

4 Results of the Comparison

Temperature, water vapour pressure and refractivity profiles observed by various radiosondes across the GBM Basin (see, Table S1) are evaluated based on those derived from COSMIC RO between August 2006 and December 2013. Of particular interest is the performance of the recently upgraded radiosondes at three stations in India: New-Delhi, Patna, and Dirbugarh, where major concerns were raised over the years (e.g., *Das Gupta et al.*, 2005; *Kumar et al.*, 2011; *Ansari et al.*, 2015). Figure S2 shows the total number of data pairs at each pressure level using the collocation criteria of 200 km radius and 2 hours time difference over the entire time period of study. The number of data pairs varied at each pressure level for both temperature and humidity (i.e., water vapour pressure) and tend to decrease rapidly with increasing altitude as most of the radiosondes burst out before reaching the stratosphere (Figure S2)

Table S1: Details of various types of radiosondes used in and around the GBM river basin between August 2006 to December 2013. The upgraded IMD radiosondes were named as GPS (Global Positioning Sytem) sondes.

SL/No	WMO ID	Make	Location/Country	Latitude	Longitude	MSL [m]	# Profiles
1	42101	IMD MK4	PATIALA/INDIA	30°20'N	76°28'E	251	1354
2	42182	GPS Sonde	NEW DELHI/INDIA	28°35'N	77°12'E	216	2937
3	42314	GPS Sonde	DIBRUGARH/INDIA	27°29'N	95°1'E	111	1687
4	42339	IMD MK4	JODHPUR/INDIA	26°18'N	73°1'E	224	1142
5	42361	IMD MK4	GWALIOR/INDIA	26°14'N	78°15'E	207	245
6	42369	IMD MK4	LUCKNOW/INDIA	26°45'N	80°53'E	128	1244
7	42379	IMD MK4	GORAKHPUR/INDIA	26°45'N	83°22'E	77	864
8	42397	IMD MK4	SILIGURI/INDIA	26°40'N	88°22'E	123	432
9	42410	IMD MK4	GAUHATI/INDIA	26°6'N	91°35'E	54	810
10	42492	GPS Sonde	PATNA/INDIA	25°36'N	85°6'E	60	1066
11	42647	IMD MK4	AHMADABAD/INDIA	23°4'N	72°38'E	55	1366
12	42667	IMD MK4	BHOPAL/INDIA	23°17'N	77°21'E	523	1011
13	42701	IMD MK4	RANCHI/INDIA	23°19'N	85°19'E	652	1248
14	42724	IMD MK4	AGARTALA/INDIA	23°53'N	91°15'E	16	681
15	42809	IMD MK4	CALCUTTA/INDIA	22°39'N	88°27'E	6	2537
16	42867	IMD MK4	NAGPUR /INDIA	21°6'N	79°3'E	310	908
17	42874	IMD MK4	RAIPUR/INDIA	21°14'N	81°39'E	298	655
18	42971	IMD MK4	BHUBANESWAR/INDIA	20°15'N	85°50'E	46	1662
19	41923	VRS92G	DHAKA/BDESH	23°46'N	90°23'E	9	843
20	41977	Unknown	CHITTAGONG/BDESH	22°21'N	91°49'E	34	210
21	41883	Unknown	BOGRA/BDESH	24°51'N	89°22'E	20	21
22	56137	Shang/M	QAMDO/CHINA	31°9'N	97°10'E	3307	908
23	55591	Shang/E	LHASA/CHINA	29°40'N	91°8'E	3650	264
24	55299	Shang/E	NAGQU/CHINA	31°29'N	92°4'E	4508	2664

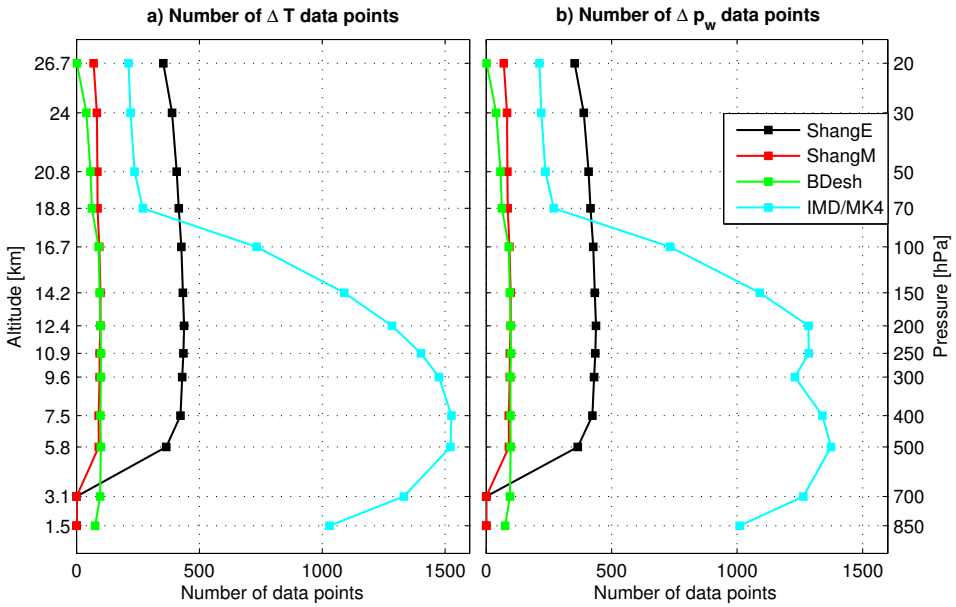

Figure S2: Number of data points at each pressure levels for temperature and humidity (water vapour pressure) of all the radiosonde types (see, Table S1) from August 2006 to December 2013.

4.1 Temperature

Figure S3 shows the temperature bias and their standard deviations of various radiosonde types in reference to the COSMIC RO data. The quality of radiosondes differ highly within the altitude range compared. Radiosondes generally show cold bias in the troposphere (below 14.2 km) and the lower

stratosphere (above the tropopause level), warm bias in the tropopause region (with the exception of radiosondes over Bangladesh). While the three radiosondes over the Bangladesh territory (labelled as "Bdesh") large (warm) bias within the UTLS region (including the tropopause), baises are generally less than ±0.5°C for those over the Chinese territory (labelled as "ShangE" and "ShangM"). ShangE appears to be better both in terms of biases (Figure S3a) and standard deviations (Figure S3b) within the tropopause even though it tend to show larger biases in the stratosphere and in the lowermost troposphere (Figure S3a). On the other hand, the radiosondes over the Indian territory (labelled as "IMD/MK4") showed the largest bias above 7.5 km (or 400 hPa level) with a standard deviation of more than 2°C (Figure S3b). These results are consistent with the most previous studies (e.g., *Sun et al.*, 2010; *Kumar et al.*, 2011; *Ansari et al.*, 2015).

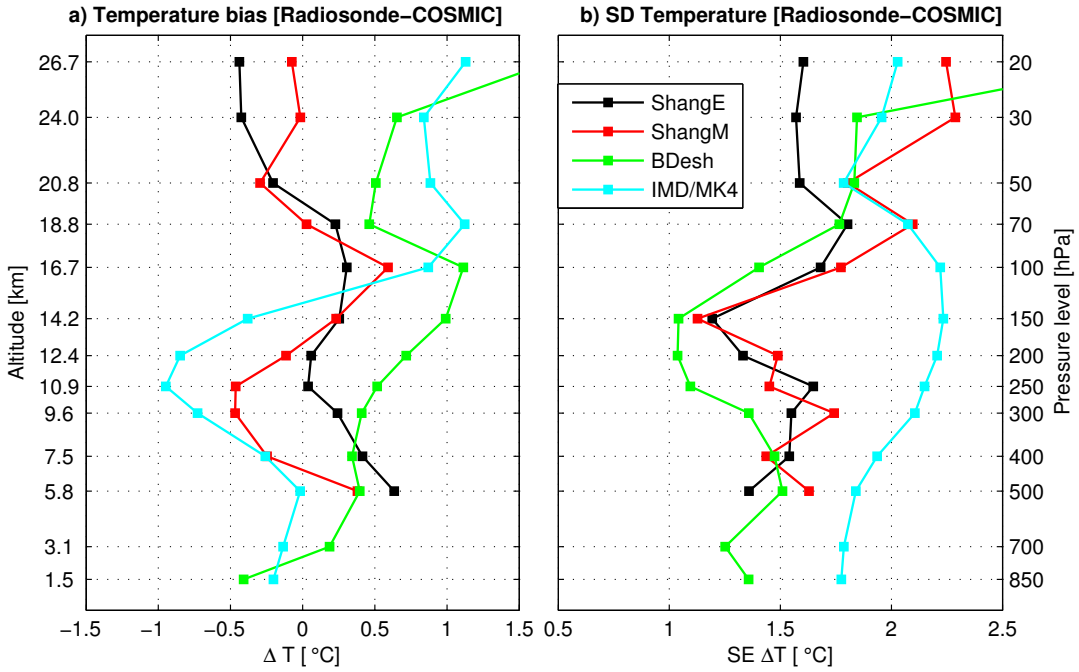

Figure S3: (a) Temperature bias and (b) standard deviations of various radiosondes (refer to Table S1) over the GBM Basin with respect to COSMIC RO data between August 2006 and December 2013.

The biases and standard deviations are calculated for the upper troposphere (400-150 hPa level) and the lower stratosphere (70-20 hPa level) separately in order to avoid the cancellation of signs and are shown in Table S2. As discussed, ShangE and ShangE shows the least temperature bias (even though of opposite signs) in both the layers. IMD/MK4 shows a cold (warm) bias of 0.6°C (1.0°C) in the upper troposphere (lower stratosphere) while the Bdesh sondes indicate warm biases in both the layers (Table S2).

In order to examine if there are any improvements at the three recently upgraded radiosonde stations (New Delhi, Patna, and Dilbugarh), a separate analysis was conducted using observations before (August 2006-May 2009) and after (June 2009-May 2013), i.e., the upgrading period. The comparison results are shown in Figure S4, which are based on more than 200 data pairs for both time periods. The analysis showed considerable improvement in temperature bias and standard deviations (see, Figure S4a-b). The large cold (warm) bias in the troposphere (stratosphere) has been largely eliminated (Figure S4a) and their variance have also been reduced substantially. GPS receivers onboard radiosondes helps to provide better estimation of pressure (in addition to geographical position) resulting in a overall improvement in its measurements. Overall, the temperature biases have reduced from -0.8°C to -0.3°C (0.6°C to 0.2°C) in the upper troposphere (lower stratosphere) as shown in Table S3. But its standard deviations are slightly higher than those shown by ShangE and ShangM radiosondes. It should be mentioned here that ShangE/M results are reported based on a relatively small sample and their biases have been reported

to be smaller than that is presented here (see, *Sun et al.*, 2010; *Wang et al.*, 2013).

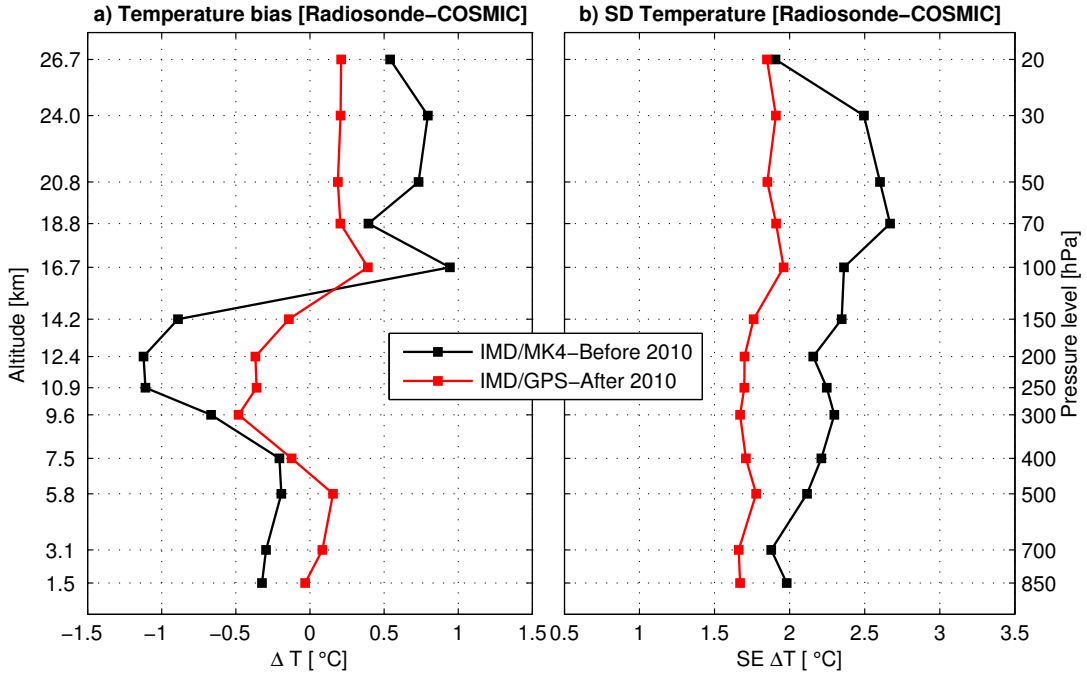

Figure S4: (a) Temperature bias and (b) standard deviations of IMD/MK4 and IMD-GPS (refer to Table S1) with respect to COSMIC RO data over the GBM Basin. The temperature biases are plotted for two periods based on three radiosonde stations (New Delhi, Patna, and Dilbugarh), one before the upgrade period (labelled as "IMD/MK4") from August 2006-May 2009 and the other after the upgrade period (labelled as "IMD/GPS") from May 2009.

Table S2: Biases in temperature, water vapour pressure, refractivity of various radiosondes used over the GBM River Basin in reference to COSMIC RO data ("wet profiles"). The statistics are computed separately for the upper troposphere (400-150 hPa) and the lower stratosphere (70-20 hPa) over the period 2006-2013.

Radiosondes	**Upper Troposphere** [400-150 hPa]			**Lower Stratosphere** [70-20 hPa]	
	ΔT [°C]	RE p_w [%]	RE N [%]	ΔT [°C]	RE N [%]
ShangE	0.2±1.5	-45.0±50.4	-0.4±0.9	-0.2±1.6	0.1±0.8
ShangM	-0.2±1.4	-35.2±47.7	-0.1±0.8	-0.1±-0.1	0±0
IMD/MK4	-0.6±2.1	-54.5±43.1	-0.1±1.2	1.0±2.0	-0.5±0.9
Bdesh	0.6±1.2	-42.4±44.4	-0.3±0.8	0.8±2.1	-0.4±1.0

Table S3: Biases in temperature, water vapour pressure, refractivity of three IMD/GPS-based radiosondes in reference to COSMIC RO data ("wet profiles"). Two statistics are calculated (see, Figure S4), one before the upgrade period (labelled as "IMD/MK4") from August 2006-May 2009 and the other after the upgrade period (labelled as "IMD/GPS") from May 2009.

Radiosondes	**Upper Troposphere** [400-150 hPa]			**Lower Stratosphere** [70-20 hPa]	
	ΔT [°C]	RE p_w [%]	RE N [%]	ΔT [°C]	RE N [%]
IMD/MK4	-0.8±2.3	-50.6±47.6	0.1±1.2	0.6±2.2	-0.3±1.0
IMD/GPS	-0.3±1.7	-35.5±50.5	-0.1±0.9	0.2±1.9	-0.1±0.9

4.2 Water Vapour

Water vapour plays an important role in the global and regional weather, climate, and hydrology but also is a major source of uncertainty in the lower troposphere (e.g., *Kuo et al.*, 2004; *Danzer et al.*, 2014). CDAAC uses a 1D-Var assimilation system to retrieve COSMIC "wet profiles" that are considered to be highly accurate (*Anthes*, 2011). Figure S5 shows the relative errors in water vapour pressure of various radiosondes with respect to the COSMIC RO ("wet profiles") data. Considering that water vapour is negligible in the stratosphere, the errors are plotted only for the troposphere (below 100 hPa level) while their statistics were computed between 400 hPa and 150 hPa. All the radiosondes show dry bias against the COSMIC RO data and their magnitudes tend to increase with altitude (Figure S5a). The biases in ShangE and ShangM sondes are found to be consistent below 200 hPa with a mean bias of -39% and 23%, respectively. Note that the relative errors shown in Table S2 are calculated between 400 hPa and 150 hPa level and it should be noted that these two radiosondes are anomalously biased at 150 hPa level.

It is also seen that IMD/GPS radonsonde show relatively lower biases above 500 hPa level (Figure S5a) and their standard deviations were also consistent around 50% (Figure S5b). The relative error has reduced by about 15% after upgrading to the GPS-based sondes at the three stations over India (see, Table S3.

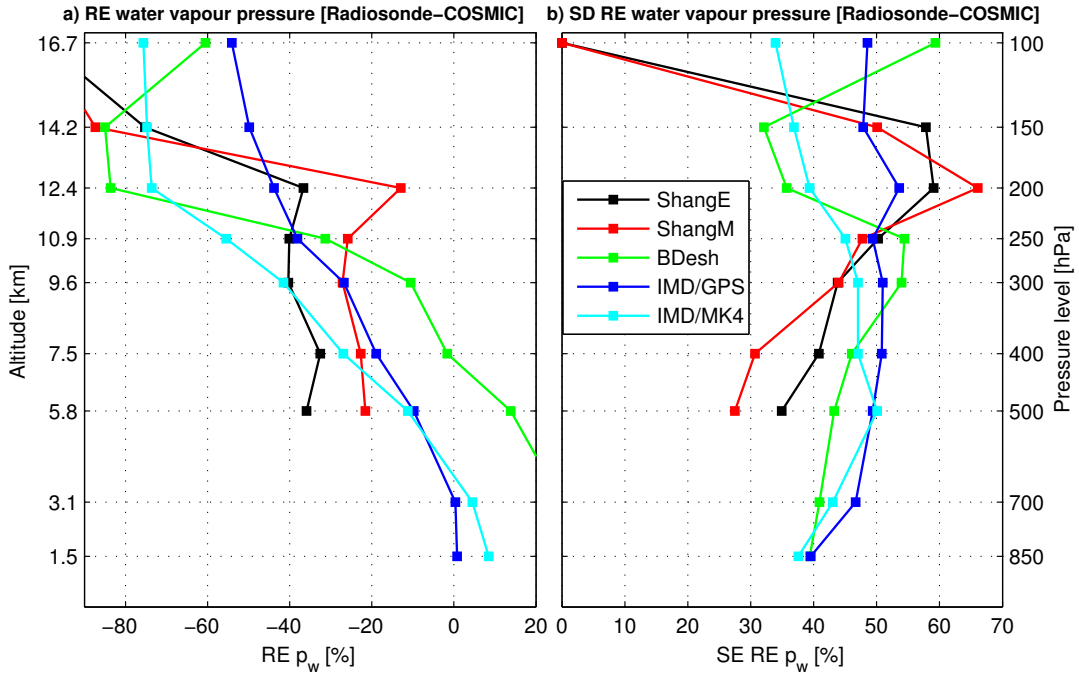

Figure S5: (a) Relative errors and (b) standard deviations of water vapour pressure (hPa) of various radiosondes over the GBM Basin with respect to COSMIC RO data.

4.3 Refractivity

Errors in refractivity are directly related to errors in observed temperatures and water vapour with the later contributing the most in the lower troposphere. The comparison results shown in Tables S2 and S3 indicated relatively large errors in temperature and water vapour pressure by IMD/MK4 and Bdesh radiosondes corresponding to very cold (warm) biases in the troposphere and stratosphere (tropopause region) (see, Figure S3a). The refractivity errors are consistent with the errors in temperature and water vapour pressure with IMD/MK4 and Bdesh radiosondes indicating the largest relative refractivity bias above 300 hPa level (FIgure S6a). However, it is seen that Bdesh radiosondes indicate the smallest

standard deviation between 300 hPa to 70 hPa level. Thus, very large refractivity errors in IMD/Bdesh sondes in the upper troposphere may have resulted from large temperature bias (see, Figure S3a).

Consistent with the temperature and water vapour pressure measurements, refractivity errors are greatly reduced in the IMD/GPS-based radiosondes both in terms of biases and standard deviations, which is now showing at par with ShangE and ShangM sondes (see Table S2 and S3).

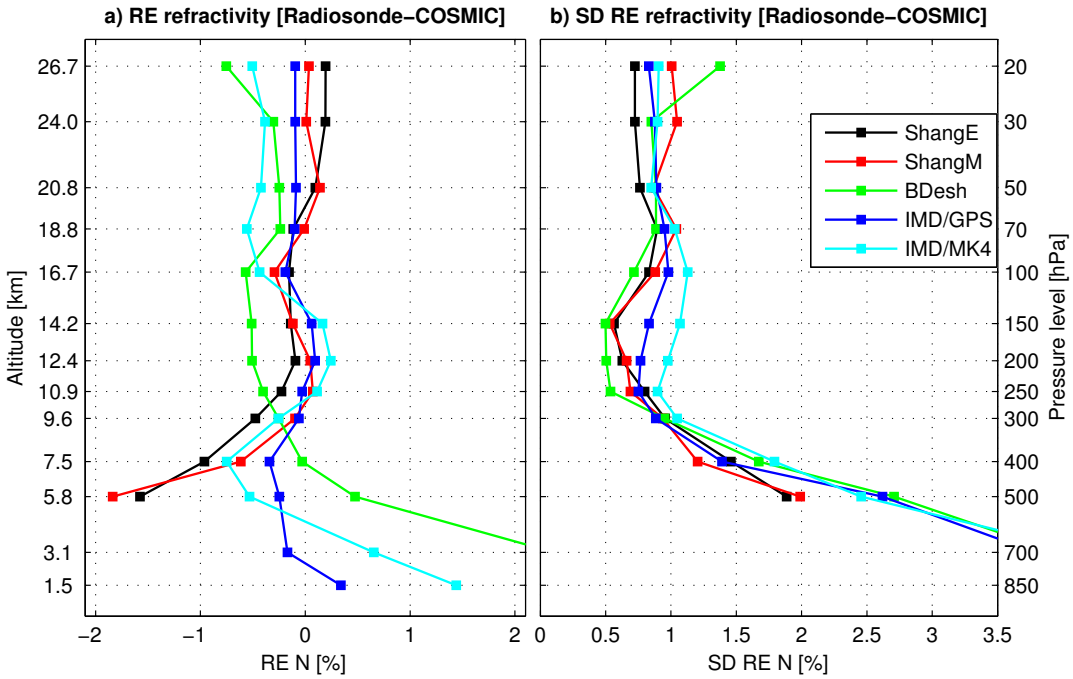

Figure S6: (a) Relative errors and (b) standard deviations of refractivity (in %) of various radiosondes with respect to COSMIC RO data over the GBM Basin between August 2006 and December 2013.

5 Interpolation of COSMIC RO data

The ordinary kriging method uses a semi-variogram to characterize the spatial variability of the variable (Z) at a point of analysis grid (x_0). The unknown value $Z(x_0)$ is interpreted as a random variable located in x_0 and is the linear combination of observed values ($z_i = Z(x_i)$) and weights $\gamma_i(x_0)$ from neighbouring locations ($i = 1, ..., N$) obtained by (e.g., *Goovaerts*, 2000):

$$\hat{Z}(x_0) = \sum_{i=1}^{N} \gamma_i(x_0) \times Z(x_i), \qquad \text{where} \sum_{i=1}^{N} \gamma_i(x_0) = 1. \tag{4}$$

An experimental semi-variogram $\hat{\gamma}(h)$ is calculated for each month as (e.g., *Goovaerts*, 2000):

$$\hat{\gamma}(h) = \frac{1}{2N(h)} \sum_{i}^{N(h)} \left[Z(x_i) - Z(x_i + h)\right]^2, \tag{5}$$

where h is the distance between two points, $N(h)$ is the number of pairs separated by distance h, $Z(x_i)$ are the observed values at x_i, and $Z(x_i + h)$ are the observed values at the next point separated by h. A theoretical semi-variogram (e.g., gaussian, spherical, exponential, etc.,) is modelled to Equation 5 to minimise the error variance and to optimise smoothing. Figure S7 shows an example of three

theoretical semi-variograms fitted to the experimental semi-variogram of COSMIC-derived tropopause temperature for September 2008. The tropopause temperature is rather spatially homogeneous over the GBM Basin for September 2008 indicating a relatively homogenous surface until about 15° (or ∼1,500 km). This indicates the scale of the atmospheric variability as opposed to a complex terrain and its associate weather in the region. Based on our experiments we have adopted the spherical model for all the months.

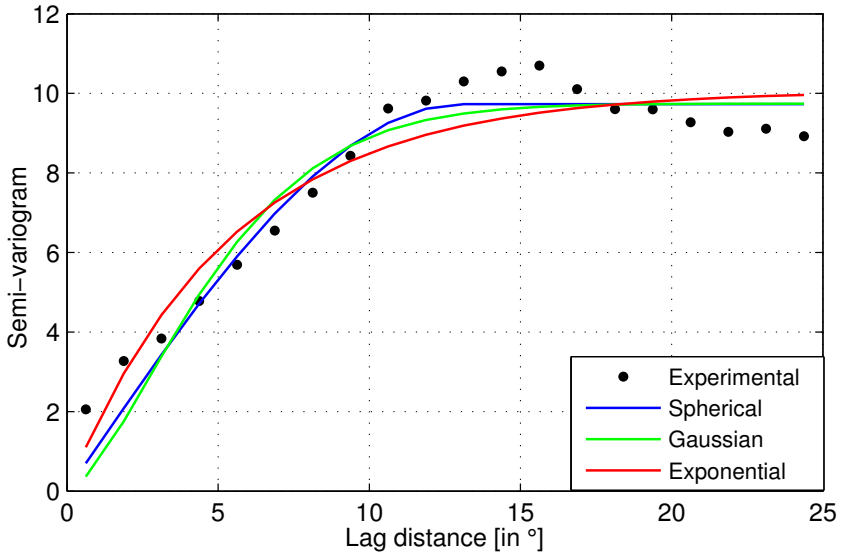

Figure S7: Semi-variogram of tropopause temperature (September 2008) over the GBM Basin based on COSMIC RO data.

References

Ansari, M. I., R. Madan, and S. Bhaita (2015), Verification of quality of GPS based radiosonde data, *Mausam*, *66*(3), 367–374, available at: metnet.imd.gov.in/mausamdocs/16632_F.pdf.

Anthes, R. A. (2011), Exploring Earths atmosphere with radio occultation: contributions to weather, climate and space weather, *Atmospheric Measurement Techniques*, *4*, 1077–1103, doi:10.5194/amt-4-1077-2011.

Danzer, J., U. Foelsche, B. Scherllin-Pirscher, and M. Schwärz (2014), Influence of changes in humidity on dry temperature in GPS RO climatologies, *Atmospheric Measurement Techniques*, *7*, 2883–2896, doi:10.5194/amt-7-2883-2014.

Das Gupta, M., S. Das, K. Prasanthi, and P. K. Pradhan (2005), Validation of upper-air observations taken during the ARMEX-I and its impact on the global analysis-forecast system, *MAUSAM*, *56*(1), 139–146.

Goovaerts, P. (2000), Geostatistical approaches for incorporating elevation into the spatial interpolation of rainfall, *Journal of Hydrology*, *228*(1-2), 113129, doi:10.1016/S0022-1694(00)00144-X.

Kumar, G., R. Madan, K. Saikrishnan, S. K. Kundu, and P. K. Jain (2011), Technical and operational characteristics of gps sounding system in the upper air network of IMD, *Mausam*, *62*(3), 403–416, available at: metnet.imd.gov.in/mausamdocs/16632_F.pdf.

Kuo, Y. H., T. K. Wee, S. Sokolovskiy, C. Rocken, W. Schreiner, D. Hunt, and R. A. Anthes (2004), Inversion and error estimation of GPS radio occultation data, *Journal of the Meteorological Society of Japan*, *82*(1B), 507–531, doi:10.1029/2004GL021443.

Sun, B., A. Reale, D. J., and D. C. Hunt (2010), Comparing radiosonde and COSMIC atmospheric profile data to quantify differences among radiosonde types and the effects of imperfect collocation on comparison statistics, *Journal of Geophysical Research*, *115*(D23), doi:10.1029/2010JD014457.

Wang, B. R., X. Y. Liu, and J. K. Wang (2013), Assessment of COSMIC radio occultation retrieval product using global radiosonde data, *Atmospheric Measurement Techniques*, *6*, 1073–1083, doi:10.5194/amt-6-1073-2013.